An observational method in time-dependent construction of thin-walled steel tanks on weak, problematic soil: A case study

Rasoul Alipour[1*], Reza Kamgar[1]

[1]Department of Civil Engineering, Shahrekord University, Shahrekord, Iran

[*] Corresponding Author: R.alipour@sku.ac.ir

ABSTRACT

This case study presents the successful application of the formal observational method to construct eighteen 2000 m³ steel storage tanks on soft, problematic soil at a port in southwestern Iran. The site investigation revealed soft clayey soils with a settlement-controlled allowable pressure of only 36 *kN/m²*, far less than the 170 *kN/m²* imposed by the proposed structures. To avoid costly deep foundations, the team implemented a geotechnical solution using engineered soil fill (2 *m*-thick, multi-layered sand, gravel, and silty gravel) placed and compacted in the tank area. Finite Element Modeling (FEM) with the Hardening Soil Model predicted a long-term consolidation settlement of 209 *mm*. A four-month controlled hydro-test was conducted to preload the ground and accelerate primary consolidation, during which tanks were interconnected with flexible polyethylene pipes to accommodate differential movements. Settlement was meticulously monitored throughout and after the hydro-test, with predefined alert, action, and alarm trigger levels as required by the observational method. Field results showed acceptable agreement with FEM predictions (average final settlement 234 *mm*). Long-term average creep after hydro-test was estimated at 30–50 *mm* over fifty years, well within the tolerance of flexible connections. The study concludes that the formal observational method, combined with soil replacement, is a viable and cost-effective strategy for such challenging ground conditions. Key practical recommendations include the use of flexible hoses for all pipe connections and sliding restraints for access ladders.

Keywords: Shallow foundations, Hydro-test, Finite Element Modeling, Bearing capacity, Field monitoring

1. Introduction

For storing palm oil, 18 steel tanks [1] of 2000 *m³* each were built in Imam Khomeini Port near the Persian Gulf, southwest Iran. The port has high ship docking fees; therefore, building storage tanks on site reduces transportation costs and delays [2, 3]. The government owns the land, but it allows private companies to build facilities at their own expense and operate them rent-free for about twenty years. Afterward, ownership of these facilities transfers back to the government. Consequently, private investors seek the lowest possible cost and shortest construction time.

Ground conditions along the Persian Gulf coast in this area include a high groundwater table (1.5 m depth), loose layers of clay, silt, and sand, low bearing capacity, and large vertical and differential settlements [4]. Additional problems include liquefaction potential, lateral spreading, and leaching of soluble minerals. In some locations, filled soils over old channels have settled nearly two meters. Conventional solutions would require deep foundations or extensive ground improvement, which are expensive and time-consuming. This reality attracts geotechnical engineers to the observational method [5-7], which can reduce costs and construction time by eliminating deep foundations [8].

The observational method is recognized in Eurocode 7 [9] but is rarely used, partly due to unclear safety definitions and lack of guidelines [10-12]. Successful applications have been reported for tanks [13], piled rafts, vacuum preloading, bridges, tunnels, dams, and embankments [14-21]. However, the designer must accept that the design may change during construction [5]. In this study, circular concrete foundations were designed to avoid general shear failure, and settlements were monitored with high precision [22]. Novel contributions of this study include: first quantitative validation of the formal observational method for a large array (18 tanks) on extremely soft clay (settlement-controlled allowable pressure 36 kPa versus imposed 170 kPa) without any deep foundations. The second one is a demonstration of how horizontal silty interlayers accelerate consolidation – a natural drainage feature rarely exploited in observational method case studies.

2. Materials and Methods

2.1 Site location

The project site is located in Imam Khomeini Port, southwest Iran (Fig. 1). The dimensions are 127.89 m × 247.99 m. Eighteen steel tanks, Eighteen steel tanks, each with a capacity of 2000 m³ (total 36,000 m³), were constructed in the first stage.

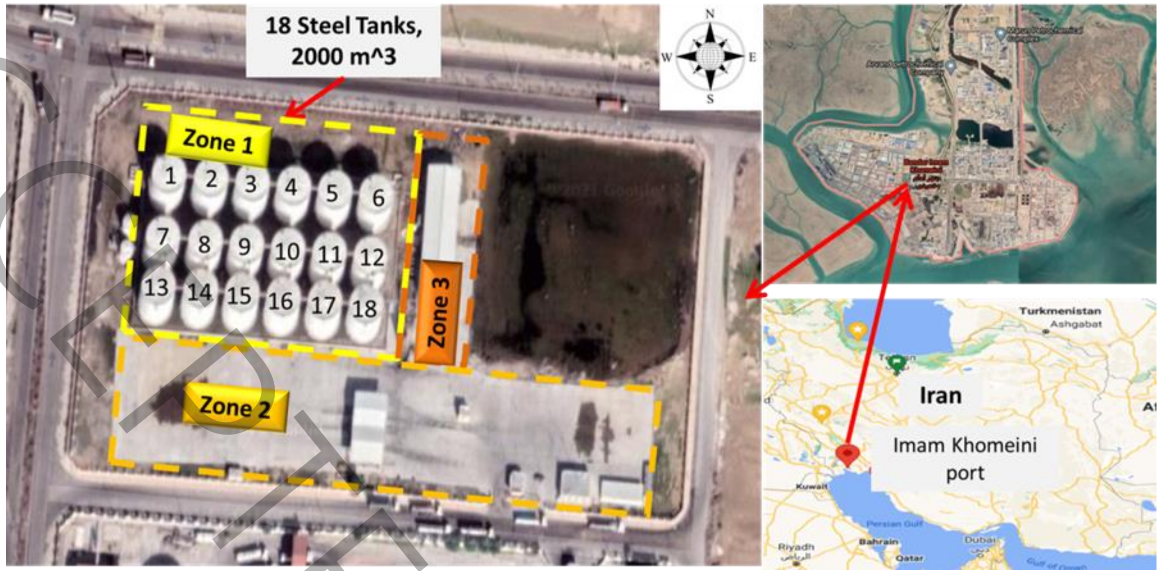

Fig. 1. Location map of 18 steel tanks

2.2 Site investigation and soil properties

Five boreholes were drilled to 40 *m* depth. Standard Penetration Tests (SPT) and laboratory tests (direct shear, triaxial, oedometer) were performed. Table 1 summarizes the soil profile to 40 *m* depth. Groundwater was encountered at 1.5 *m*. The near-surface soils are clay with low plasticity (CL), interbedded with silty layers (ML) at depths of 1.5–3 *m*, 13–16 *m*, and 30–34 *m*. These silty layers act as horizontal drains, accelerating consolidation.

Table 1. General characteristics of subsurface soil layers (0–40 *m* depth)

Depth, m	Soil type	LL	PI	C_{uu}, (kPa)	Φ_{uu}, (°)	Wn, %	e_0	Cc	Cr	SPT
0-1.5	CL	32	38	0.45	4	36.08	0.70	0.13	0.01	12
1.5-3	ML	--	--	0.42	30	--	--	--	--	14
3-5	CL	34	18	0.44	4	36.08	0.724	0.13	0.01	15
5-7	CL	33	19	0.45	4	35.09	0.714	0.14	0.01	16
7-10	CL	34	19	0.50	5	35.07	0.712	0.16	0.01	10
10-13	CL	32	18	0.49	5	35.16	0.701	0.15	0.01	13
13-16	ML	--	--	--	--	33.92	--	--	--	27

16-18	CL	31	19	0.55	5	32.47	0.687	0.11	0.00	24
18-20	CL	31	18	0.53	5	32.68	0.688	0.12	0.01	24
20-23	CL	33	19	0.56	5	29.55	0.685	0.10	0.01	30
23-27	CL	30	18	0.62	6	31.98	0.684	0.10	0.01	28
27-30	CL	34	18	0.59	5	31.99	0.682	0.09	0.01	31
30-34	ML	--	--	0.65	6	--	--	--	--	24
34-38	CL	34	19	0.61	5	28.01	0.606	0.09	0.01	31
38-40	CL	30	18	0.58	5	32.01	0.685	0.11	0.01	24

Water level= 1.5m

The settlement-controlled allowable pressure for a shallow circular foundation (diameter 15.85 *m*) with settlement controlled to 4 in (101.6 *mm*) was only 36 kPa at 1 *m* depth (Fig. 2).

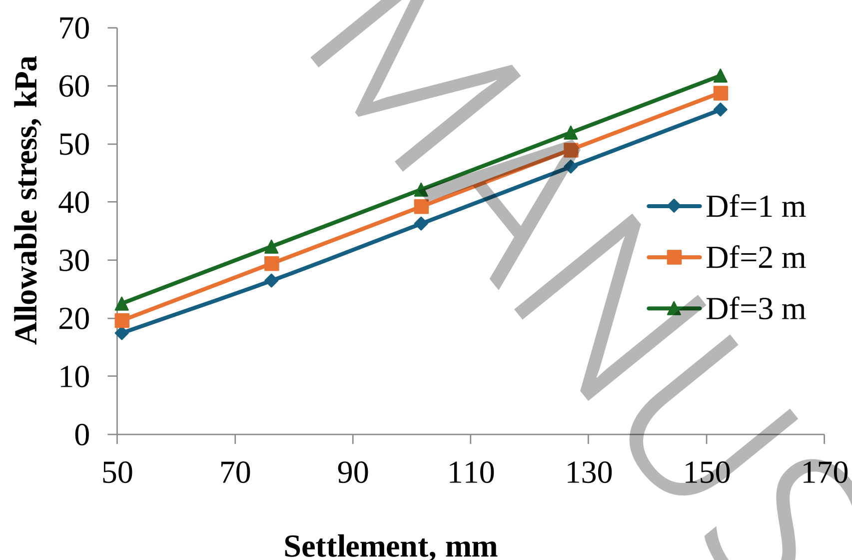

Fig. 2. Settlement vs. allowable stress for circular foundation

2.3 Imposed stress beneath the circular foundations

Each tank has a circular concrete foundation of diameter 15.85 *m* (area 197.21 m^2). The total vertical load includes:

- Steel tank (bottom plate, roof, walls, accessories): 1037.6 *kN*

- Palm oil (specific gravity 0.916, but hydro-test [18] uses water at 1.0): during operation 18731 *kN*; during hydro-test 20434 *kN*

- Concrete foundation: 2901 *kN*

The stress beneath the foundation during hydro-test is:

$$\sigma = \frac{1037.6 + 20434 + 2901}{197.21} = 123.58\ kPa \tag{1}$$

It is critical to clarify that the 36 *kPa* value is the allowable bearing pressure derived strictly from the settlement serviceability criterion (4 inches / 101.6 *mm*), not the ultimate bearing capacity. To verify the safety against a bearing-capacity (shear) failure, we calculated the ultimate bearing capacity using the Meyerhof method for a circular footing (diameter D = 15.85 *m*, embedment depth Df = 1.0 *m*). The applied stress of 163 *kPa* used in this bearing-capacity verification corresponds to the stress at the interface between the engineered fill and the underlying natural clay (i.e., at the base of the 2 *m* soil replacement layer), which accounts for the tank and foundation load (123.6 *kPa* from Eq. 1) plus the self-weight of the overlying 2 *m* engineered fill. Using the drained strength parameters of the underlying clay (c' = 10 *kPa*, φ' = 25°) and unit weight (γ = 16 kN/m^3), the ultimate bearing capacity was estimated as q_{ult} = 420 *kPa*. This provides a factor of safety of FoS = q_{ult} / $q_{applied}$ = 420 / 163 = 2.6 against the maximum hydro-test loading. Thus, the observational method and soil replacement were implemented primarily to mitigate excessive consolidation settlement, rather than to prevent an imminent bearing-capacity failure.

2.4 Engineering soil filling (zoning)

To increase bearing capacity and prevent general shear failure, the site was divided into three zones (Fig. 1 and Fig. 3):

Zone 1 (under tanks): 2 m thick engineered fill. After removing the weak surface sludge, a 350 *mm* saturated sand layer (compacted to 1.7 g/cm^3) was placed, followed by 750 *mm* of poorly graded gravel (GP), then 150 *mm* lifts of silty gravel (GM) compacted to 98% of modified Proctor density (ASTM D1557).

Zone 2 (access roads and loading areas): 1.35 *m* thick fill (500 *mm* sand, 400 *mm* GP, 450 *mm* GM).

Zone 3 (building area): 1.15 *m* fill.

Figure 3 shows the filling sections.

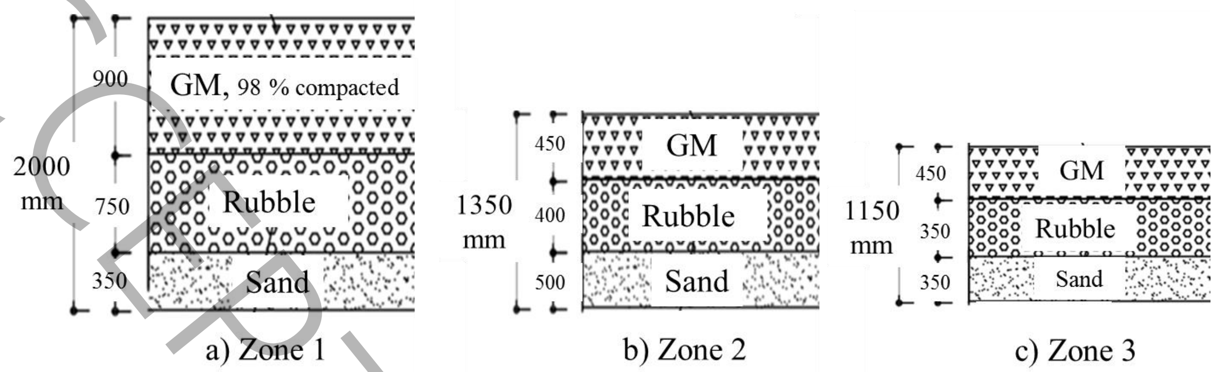

Fig. 3. Soil filling sections in different zones

Figure 4 shows Grain size distribution curves of CL, SP, GP, and GM. Table 2 summarizes GM layer properties, including California Bearing Ratio (CBR), swelling, and maximum dry density.

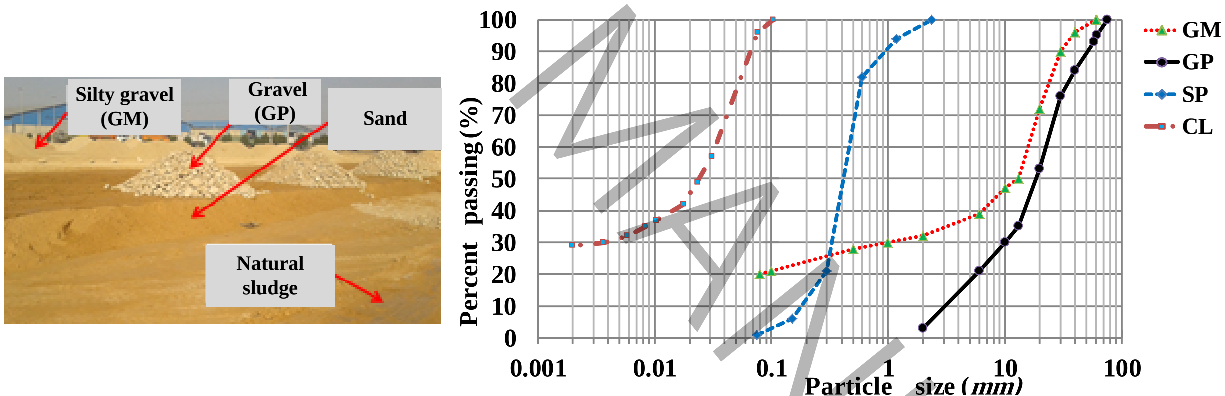

Fig. 4. Grain size distribution curves

Table 2. Summarizes GM layer properties (California Bearing Ratio, swelling, maximum dry density)

		Sample 1	Sample 2	Sample 3
Maximum dry density, gr/cm^3		1.99	2.00	2.01
Optimum water content, %		11.3	11.50	11.30
Soil type		GM	GM	GM
CBR, saturated	Ten blow count	2	2	2
	Swelling after 96 hours, %	0.18	0.23	0.15
CBR, saturated	30 blow count	6	7	5
	Swelling after 96 hours, %	0.13	0.16	0.12
CBR, saturated	65 blow count	10	11	9
	Swelling after 96 hours, %	0.07	0.09	0.09

2.5 Plate load tests

Six plate load tests [23] were performed on the compacted GM layer to verify quality. The average subgrade reaction modulus (k_s) was 0.092 *N/mm³*. Figure 5 shows the results of the PLT.

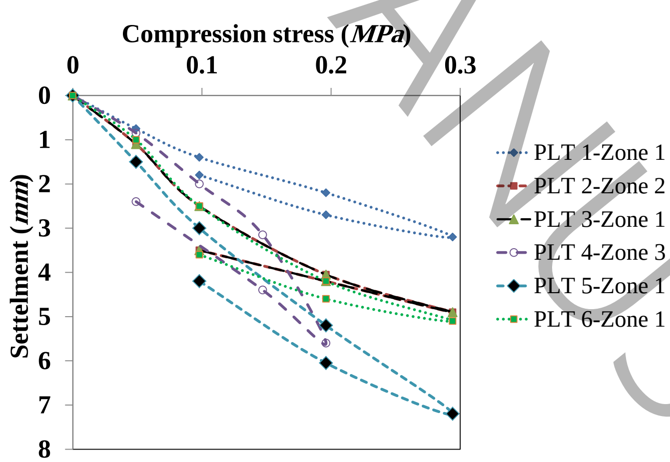

Fig. 5. PLT load-settlement curves and test setup

2.6 Finite Element Modeling (FEM)

2.6.1 Model geometry and boundary conditions

A two-dimensional plane strain finite element model was developed using PLAXIS 2D [24]. Although each steel tank is circular in plan, the project comprises 18 tanks arranged in three parallel rows (north, middle, south) with six tanks per row. The critical geotechnical behavior (vertical and differential settlement) occurs primarily in the longitudinal direction of each row, where adjacent tanks interact . Therefore, a plane strain cross-section perpendicular to the tank rows (i.e., cutting through the centerline of a row) adequately captures the consolidation and settlement patterns. This approach is standard in geotechnical practice for tank farms and embankments, where the length of the loaded area (row of tanks) is much greater than its width. Plane strain may under-predict settlement; indeed, the measured average settlement (234 *mm*) was approximately 12% higher than the FEM prediction (209 *mm*), which is acceptable for this type of analysis.

The model domain extends 50 *m* in depth and 300 *m* in width (horizontal direction). The bottom boundary is fixed in both vertical and horizontal directions. The vertical lateral boundaries are fixed horizontally but free vertically to allow settlement. Fifteen-node triangular elements were used for all soil layers. Figure 6 shows the geometrical model of the tank row and soil strata.

The adopted plane-strain formulation entails a geometric simplification in which the discrete circular footprints of the tanks are represented as a continuous strip load. This approximation is well-justified by the overall length-to-width ratio of the tank farm (~5:1) for the first-order estimation of average vertical settlements. However, the plane-strain model inherently precludes the accurate simulation of three-dimensional stiffening effects and localized load-transfer mechanisms between adjacent circular footings. Consequently, this intrinsic limitation tends to produce an underestimation of differential settlements, as discussed in Section 3.4. While a full three-dimensional consolidation analysis would offer enhanced predictive fidelity, it was not pursued in the present study owing to practical computational resource constraints. Nevertheless, for the primary engineering objective, namely, estimating the magnitude and rate of average consolidation settlement to establish the preloading schedule. The plane-strain model yielded sufficiently reliable and practically applicable guidance.

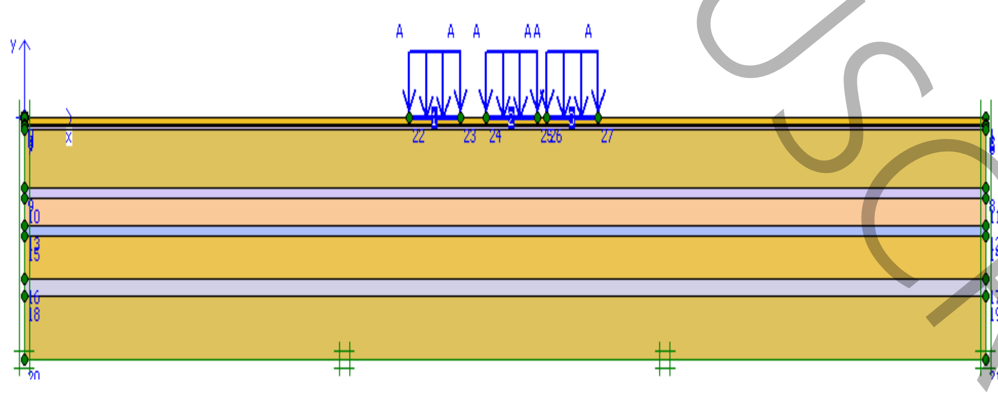

Fig. 6. Modeling of reservoirs and soil layers in finite element method

2.6.2 Constitutive models and parameters

Soft clay layers (CL and ML) were modeled with the Hardening Soil Model with small-strain stiffness (HSsmall) to capture both primary consolidation and small-strain behavior under working loads. Table 3 lists the HSsmall parameters for each soil layer, calibrated from oedometer and triaxial tests.

Table 3. HSsmall parameters

Soil type	Depth (m)	γ_{unsat} (kN/m³)	γ_{sat} (kN/m³)	E_{50ref} (MPa)	E_{oedref} (MPa)	E_{urref} (MPa)	m	c' (kPa)	φ' (°)	ψ (°)	R_f	G_{0ref} (MPa)	$\gamma_{0.7}$ (×10⁻⁴)	k_v (m/day)	k_h (m/day)
CL	0 – 1.5	16.0	18.5	2.8	2.2	8.4	0.9	10	25	0	0.9	40	2.5	2.5×10^{-4}	3.0×10^{-4}
ML	1.5 – 3	15.5	18.0	4.5	3.8	13.5	0.8	5	28	0	0.9	65	2.0	1.2×10^{-3}	2.5×10^{-3}
CL	3 – 5	15.8	18.2	3.0	2.4	9.0	0.9	12	26	0	0.9	45	2.4	2.0×10^{-4}	2.5×10^{-4}
CL	5 – 7	15.8	18.2	3.2	2.5	9.6	0.9	12	26	0	0.9	48	2.4	2.0×10^{-4}	2.5×10^{-4}
CL	7 – 10	15.9	18.3	3.3	2.6	9.9	0.9	13	27	0	0.9	50	2.3	2.0×10^{-4}	2.5×10^{-4}
CL	10 –13	16.0	18.3	3.4	2.7	10.2	0.9	13	27	0	0.9	52	2.3	2.0×10^{-4}	2.5×10^{-4}
ML	13–16	15.5	18.0	5.0	4.2	15.0	0.8	5	28	0	0.9	70	2.0	1.0×10^{-3}	2.2×10^{-3}
CL	16–18	16.0	18.4	3.8	3.0	11.4	0.8	14	28	0	0.9	55	2.2	1.8×10^{-4}	2.2×10^{-4}
CL	18–20	16.1	18.4	3.9	3.1	11.7	0.8	14	28	0	0.9	56	2.2	1.8×10^{-4}	2.2×10^{-4}
CL	20–23	15.9	18.1	3.5	2.8	10.5	0.9	15	29	0	0.9	53	2.3	1.8×10^{-4}	2.2×10^{-4}
CL	23–27	15.9	18.0	3.6	2.9	10.8	0.9	15	29	0	0.9	54	2.3	1.8×10^{-4}	2.2×10^{-4}
CL	27–30	16.0	18.1	3.7	3.0	11.1	0.9	15	30	0	0.9	55	2.3	1.8×10^{-4}	2.2×10^{-4}
ML	30–34	15.5	18.0	5.5	4.5	16.5	0.8	5	29	0	0.9	72	2.0	9.0×10^{-4}	2.0×10^{-3}
CL	34–38	16.2	18.5	4.0	3.2	12.0	0.8	16	31	0	0.9	58	2.2	1.8×10^{-4}	2.2×10^{-4}
CL	38–40	16.0	18.3	3.9	3.1	11.7	0.8	14	28	0	0.9	56	2.2	1.8×10^{-4}	2.2×10^{-4}

Table 4 illustrates that engineered fill (GM) and gravel layers (GP) were modeled with the Mohr-Coulomb model because of their granular, non-creeping behavior.

Table 4. Mohr Coulomb parameters in engineered fills

Material	γ_{unsat}, (kN/m³)	γ_{sat}, (kN/m³)	E, (MPa)	ν	c' (kPa)	φ' (°)	ψ (°)
Sand (SP)	16.5	19.0	25	0.3	0	34	4
Poorly graded gravel (GP)	17.0	20.0	40	0.28	0	38	6
Silty gravel (GM)	17.5	20.5	45	0.27	5	36	5

2.6.3 Mesh sensitivity analysis

Three meshes were tested, including coarse, medium, and fine types. The results of the mesh sensitivity analysis are presented in Table 5.

Table 5. Mesh sensitivity analysis

Mesh size	Element numbers	Predicted settlement, mm
Coarse	2100	221
Medium	3800	209
Fine	5200	205

The change from medium to fine was less than 2%. The medium mesh was adopted for all analyses.

2.6.4 Consolidation and creep modeling

Time-dependent consolidation was modeled using Biot's coupled formulation with laboratory-measured permeabilities. Secondary compression (creep) was assessed separately using the secondary compression index C_α determined from long-term oedometer tests ($C_\alpha/C_c \approx 0.03$ for these clays). The hydro-test duration (120 days) was designed to achieve approximately 85% primary consolidation at the end of water filling; however, this plan was altered during implementation.

2.7 Structural design of circular foundations

The circular mat foundation (diameter 15.85 *m*, thickness 0.7 *m*) was designed in SAFE software. Figure 7 shows the cross-section and details of 16 jack slots used for future leveling if differential settlement exceeded tolerances.

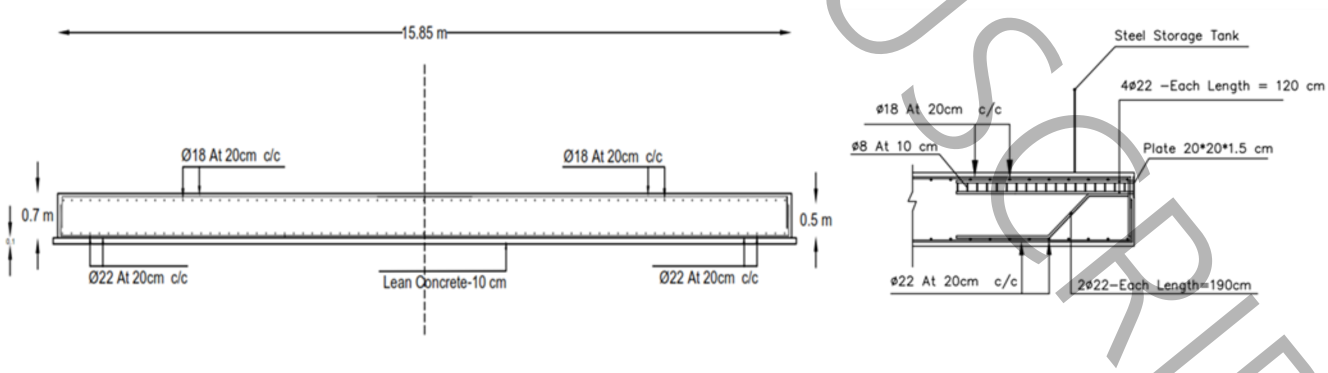

a) Cross section of circular mat foundation

b) Jack slot (total no=16)

Fig. 7. Circular mat foundation of tanks; a) Transverse section of the circular foundation, b) details for 16 jack slots

2.8 Formal application of the Observational Method

Following Peck [5] and Eurocode7 [9], the following trigger levels and contingency plans were defined before construction in Table 6.

Table ٦. Trigger levels and contingency plans

Trigger level	Criterion	Action/Contingency Plan
Alert	Differential settlement > 30 *mm* (≈ 1/300 slope) OR Uniform settlement rate > 2 mm/day for 5 consecutive days.	Increase monitoring frequency to daily; inspect flexible hoses and ladder connections for visual distortion.
Action	Differential settlement > 50 *mm* (≈ 1/200 slope, per API 650) OR Uniform settlement > 100 mm (50% of total tolerance).	Pause hydro-test filling; notify the purchaser; prepare jack slots for potential leveling; perform additional plate load tests.
Alarm	Settlement rate > 5 mm/day for 3 consecutive days OR Total settlement >150 *mm* before reaching 50% of the maximum fill height.	Stop hydro-test immediately; depressurize tanks if necessary; install temporary internal steel bracing; consider staged filling or installation of granular drainage columns if the rate does not stabilize within 14 days.

The contingency plans comprised three pre-designed physical intervention stages: (i) temporary internal steel bracing, to be deployed if tilting exceeded 0.5°; (ii) installation of granular drainage columns, if the settlement rate failed to decrease after 14 days of maintaining a constant water level; and (iii) utilization of jack slots (Fig. 7b) to re-level the foundation, should differential settlement surpass 50 mm after completion of the hydro-test.

Although these three physical contingency measures were never ultimately implemented, their formal definition satisfied the requirements of the observational method. However, it is important to note that the monitoring data did indicate that the Alert and Action thresholds (Table 6) for both uniform and differential settlements were indeed exceeded during filling. Consequently, the procedural responses corresponding to these levels (i.e., increased monitoring frequency and a temporary pause in hydro-test filling) were activated. Crucially, the Alarm threshold was never reached.

The decision not to escalate to the physical contingency measures was justified because the reservoir stores non-hazardous and non-flammable palm oil. For this specific project, the observed elevated settlements were evaluated and deemed acceptable, provided that: (a) no general shear failure occurred in the foundation soil, and (b) the flexible nature of the tank connections tolerated the measured differential movements.

2.9 Hydro-test procedure

Each tank was filled with water following the diagram in Fig. 8 (120-day schedule). The filling rate was controlled to avoid undrained failure. Flexible polyethylene pipes (able to tolerate up to 250 *mm* vertical displacement) connected adjacent tanks during the test (Fig. 9a). Settlement benchmarks were installed on the north, south, east, and west sides of each tank (Fig. 9b). Monitoring continued for up to 912 days after the start of the hydro-test.

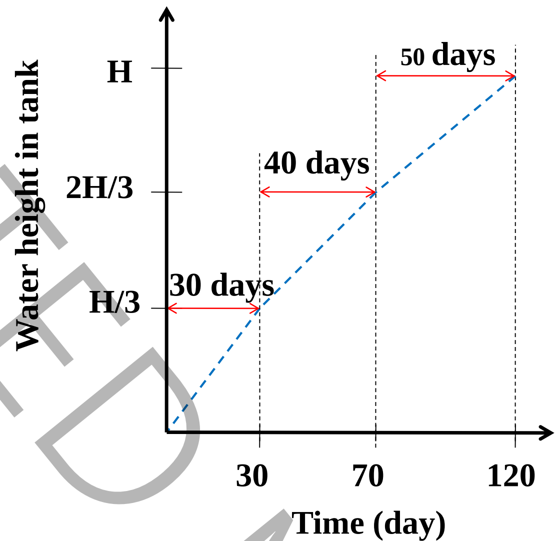

Fig. 8. Hydro-test filling diagram – height vs. time

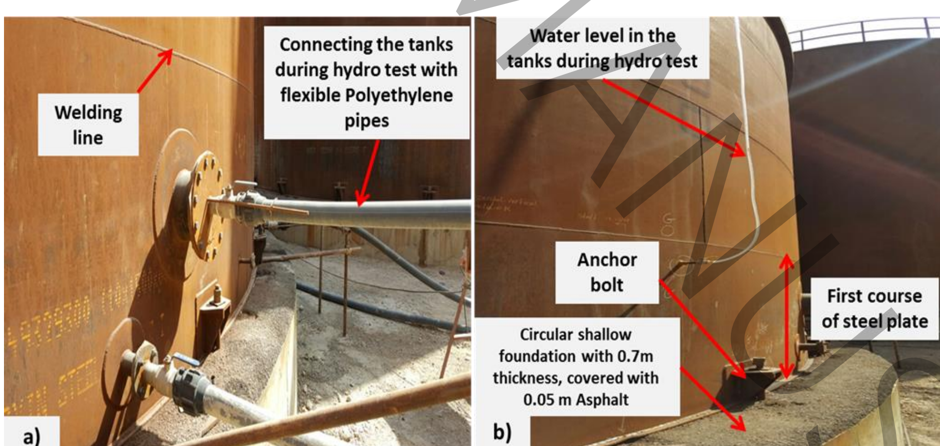

Fig. 9. Hydro-test process: a) setup of polyethylene pipes during the hydro-test, b) settlement monitoring with controlling water level

This hydro-test plan was changed during implementation, as described in Section 3.3.

3. Results

3.1 Definitions

The following definitions should be considered for various terms of settlement.

Settlement after hydro-test (S_h), measured immediately after the 4-month water filling and draining.

Final settlement (S_f), measured at the end of the monitoring period (up to 912 days after hydro-test start).

Tolerable settlement during operation, S_f-S_h (additional settlement that flexible connections must accommodate).

3.2 FEM-predicted settlements

Figure 10 (plane strain FEM) shows predicted vertical settlement in the north-south direction. Maximum settlement is 209 *mm* at the center of the tank group.

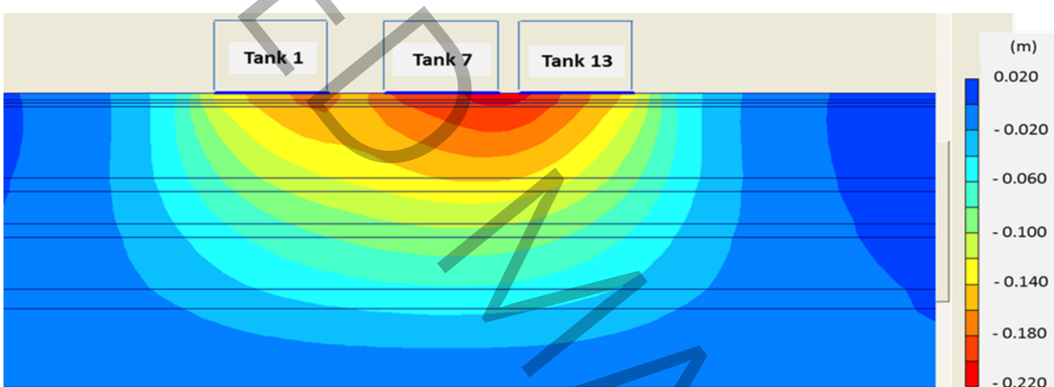

Fig. 10. FEM vertical settlement contours, N-S direction

In the east-west direction, the maximum vertical settlement is 208 *mm* (Fig. 11). The maximum differential settlement predicted by FEM was 51.1 *mm* (south tanks, N-S direction).

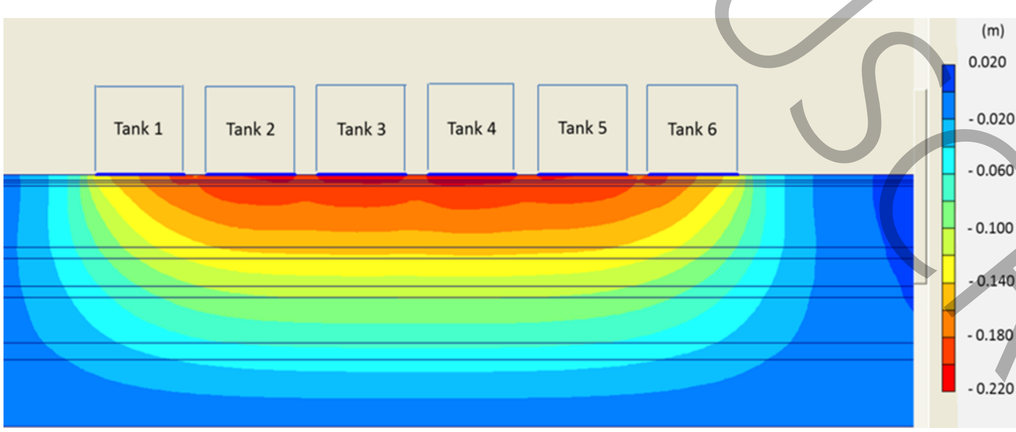

Fig. 11. FEM vertical settlement contours, E-W direction

3.3 Field monitoring results

The hydro-test started on different dates for the three rows:

- North tanks (Nos. 1–6): started May 30, 2016; test duration: 116 days.

- Middle tanks (Nos. 7–12): started April 16, 2016; duration 74 days.

- South tanks (Nos. 13–18): started July 10, 2016; duration 95 days.

Table 7. Average vertical settlement of steel tanks after hydro-test and during operation

Tank no	Hydro-test time, days	Average settlement after finishing hydro-test, S_h (*mm*)	Monitoring time from starting hydro-test, days	Final Settlement minus Settlement after finishing hydro-test, S_f-S_h (*mm*)
1	116	211	912	16
2	116	202	912	26
3	116	223	912	26
4	116	223	912	16
5	116	222	912	26
6	116	204	912	9
7	74	167	880	36
8	74	173	880	56
9	74	187	880	45
10	74	182	880	36
11	74	180	880	26
12	74	177	880	16
13	95	176	772	76
14	95	181	772	76
15	95	199	772	86
16	95	189	772	66

17	95	185	772	56
18	95	180	772	56

Table 7 presents average settlement values after hydro-test and final settlement for each tank. The larger values in Table 7 include remaining primary consolidation, and 30–50 *mm* over 50 years refers only to secondary (creep) settlement. The key findings of average vertical settlements are:

- Maximum S_h: 223 mm (tanks 3 & 4, north row)

- Maximum S_f: 285 mm (tank 15, middle row)

- Maximum S_f-S_h (tolerable settlement): 86 *mm* (tank 15), within the flexible hose tolerance (250 *mm*).

For each tank, four benchmarks were established on the circular mat foundation at its north, south, east, and west sides during the monitoring stage. Figures12-14 depict the maximum vertical settlement for each tank.

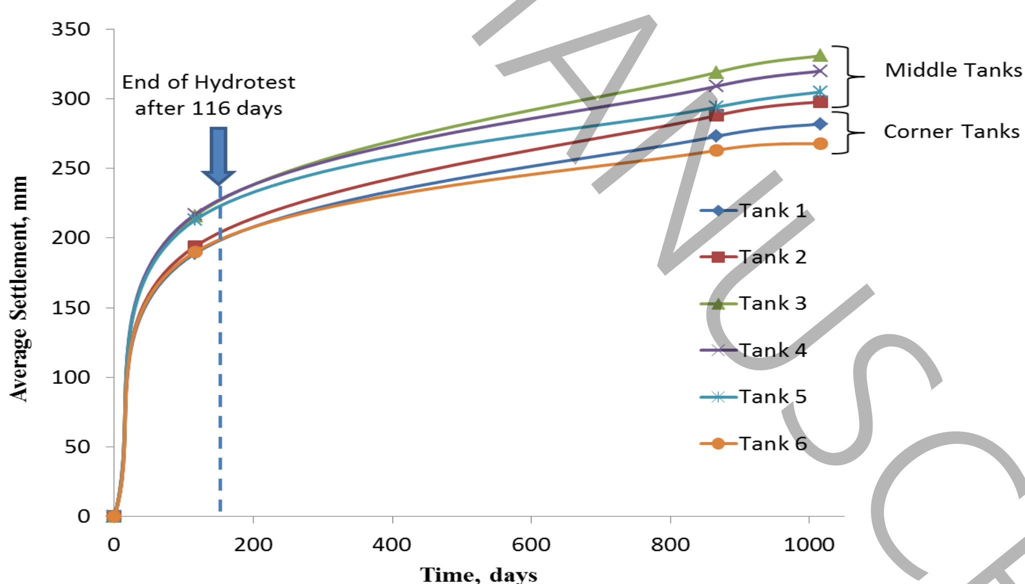

Fig. 12. Vertical maximum settlement of circular foundation in tanks 1 to 6 (North tanks).

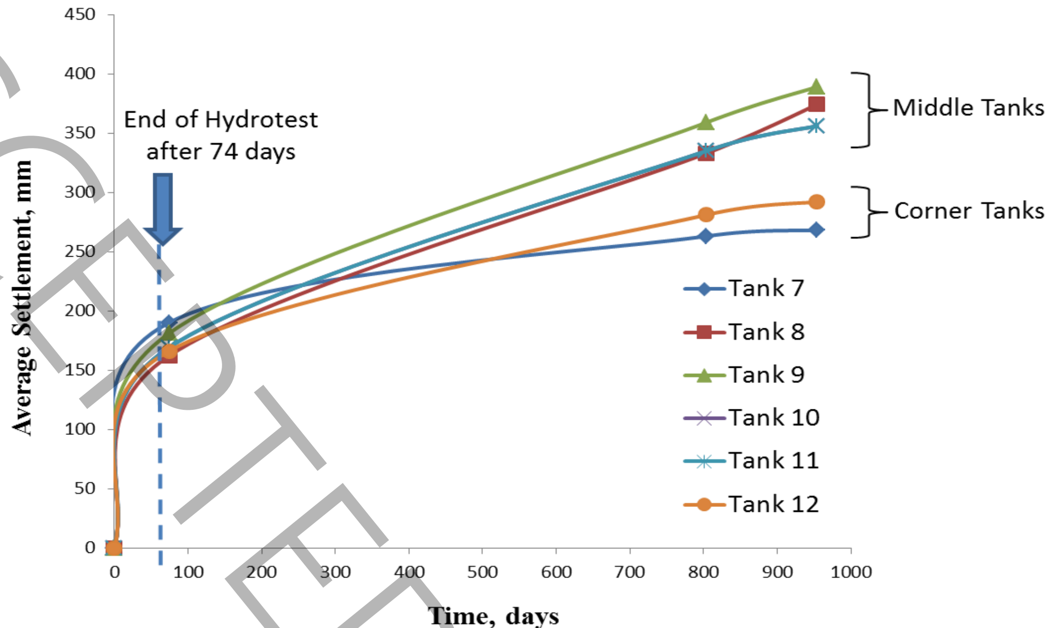

Fig. 13. Vertical maximum settlement of circular foundation in tanks 7 to 12 (middle tanks).

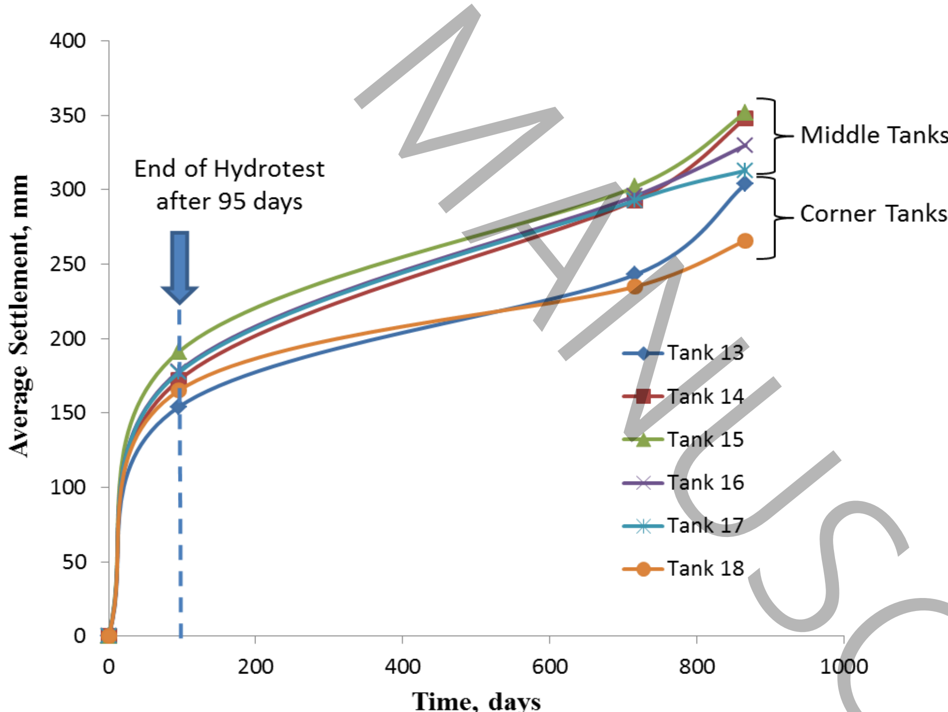

Fig. 14. Vertical maximum settlement of circular foundation in tanks 13 to 18 (South tanks).

Figures 15–17 show differential settlement per tank row. Maximum differential settlement in the N- S direction was 89 *mm* (tank 9). In the E-W direction, it was 86 *mm* (tank 7). Both exceeded the FEM prediction of 51 *mm* but were accommodated by flexible hoses and jack slots.

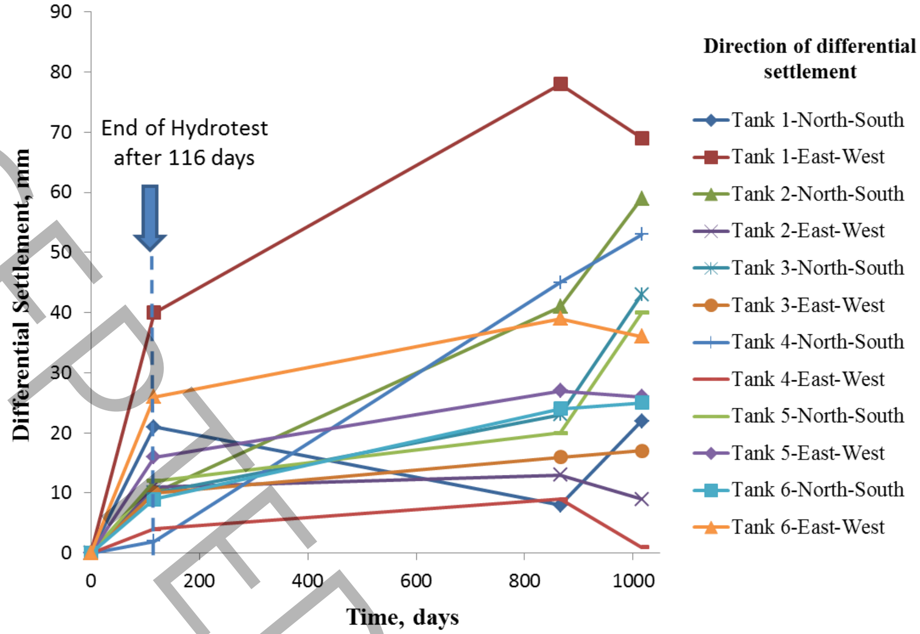

Fig. 15. Differential settlement of circular foundation in tanks 1 to 6 (North tanks).

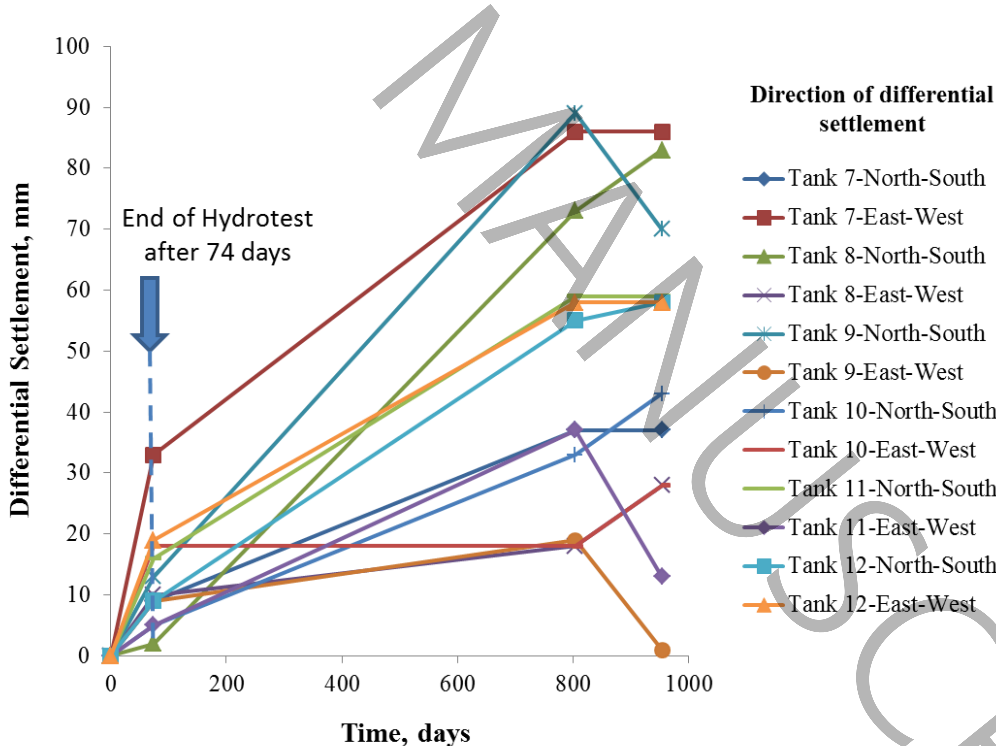

Fig. 16. Differential settlement of circular foundation in tanks 7 to 12 (middle tanks).

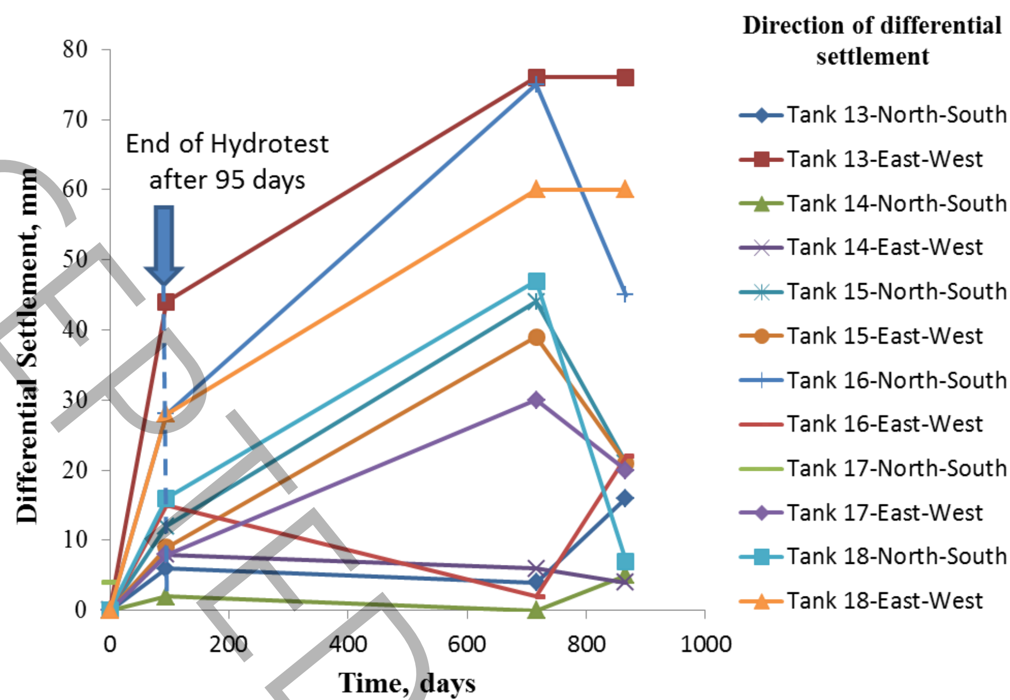

Fig. 17. Differential settlement of circular foundation in tanks 13 to 18 (South tanks).

3.4 Comparison of FEM predictions with field measurements

Tank-by-tank comparison of FEM and monitoring results for vertical settlement is illustrated in Fig. 18. The average measured final settlement (234 *mm*) is approximately 12% higher than the FEM prediction (209 *mm*), which is considered acceptable given natural soil variability and the numerical modelling.

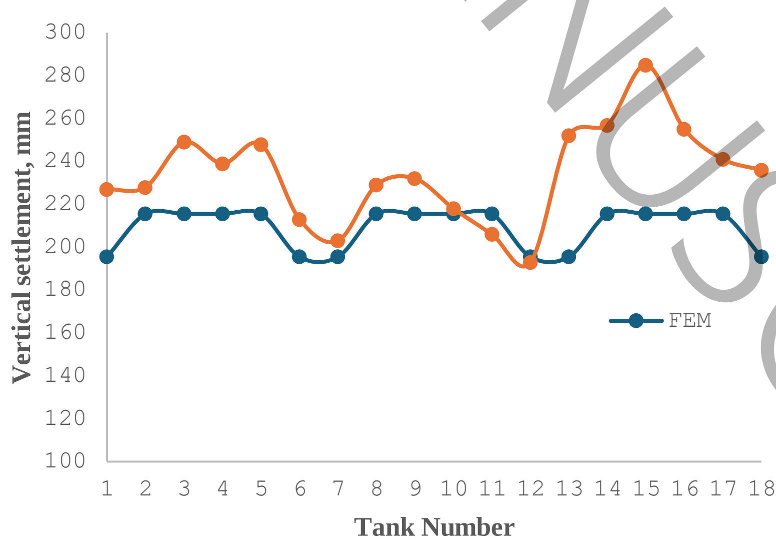

Fig. 18. Tank-by-tank comparison of FEM and monitoring results for vertical settlement.

In contrast, the differential settlement was significantly under-predicted by the FEM: the model predicted 51 mm, while field measurements recorded up to 89 *mm*. Relative to the measured value, this corresponds to a 43% under-prediction (i.e., the FEM captured only 57% of the observed differential movement). We acknowledge that this level of accuracy is insufficient for rigorous quantitative validation of differential movements.

This under-prediction is attributed to: (a) the inherent spatial variability of the soft clay layers, which is not captured by the deterministic HSsmall model; (b) the plane-strain idealization (Section 2.6.1), which enforces a continuous load distribution and cannot replicate the true 3D interaction between adjacent circular foundations; and (c) minor localized variations in the compaction quality of the granular fill.

Despite this poor quantitative prediction, the design remained safe and fully functional because the measured differential settlements (89 *mm*) remained substantially below the 250 *mm* serviceability tolerance of the flexible polyethylene hoses. Furthermore, the provision of jack slots (Section 2.8) offers an additional margin for future re-leveling if required.

4. Discussion

4.1 Performance of the observational method

The Alarm threshold (Table 6) was never exceeded during the hydro-test; consequently, the three physical contingency plans (steel bracing, drainage columns, and jack-slot leveling) were not deployed. However, the Alert and Action monitoring levels were temporarily triggered (as discussed in Section 2.8), requiring increased monitoring frequency and a temporary pause in filling, demonstrating that the observational method functioned as intended. The hydro-test was completed safely, and the predefined contingency framework satisfied the requirements of Eurocode 7 [9].

The implemented solution, comprising a 2 *m* soil replacement layer, an extended hydro-testing period, and the associated monitoring, cost approximately \$1.7 million. At the tendering stage, a conventional driven precast concrete pile alternative (designed to transfer loads to the deeper stiffer layer at 30 *m* depth) was priced at approximately \$2.8 million USD. This yields a direct cost saving of roughly 40% (calculated as $(2.8 - 1.7) / 2.8 \approx 40\%$). Additional savings from the reduced construction schedule (compared to pile installation) are not included in this estimate.

Client-imposed scheduling constraints affected a reduction in the hydro-test window. Accelerated filling would have reduced the effectiveness of the preloading and increased the risk of long-term differential settlement, a lesson that reinforces the value of strictly adhering to the observational method.

4.2 Role of silty interlayers in consolidation

The three ML layers at depths 1.5–3 *m*, 13–16 *m*, and 30–34 *m* acted as horizontal drains, effectively shortening the vertical drainage paths. To quantify this effect, a parametric FEM study was conducted in which the three ML layers were artificially assigned the hydraulic conductivity and compressibility of the surrounding CL clay, effectively creating a 'homogeneous clay' scenario for comparison.

In this homogeneous scenario, the time required to reach 85% primary consolidation under hydro-test loading increased from 90 days to 125 days. This corresponds to a 28% reduction in preloading duration (computed as 1−(90/125)= 28%).

It should be noted that this parametric comparison captures the net effect of replacing the silty layers with clay, which simultaneously alters both the drainage characteristics and the overall compressibility of the soil profile. However, the dominant contribution to the observed 28% time saving is attributed to the horizontal drainage provided by the high-permeability ML layers, as the shortened drainage paths are the primary mechanism governing pore-pressure dissipation in stratified soft deposits. This confirms that these silty interlayers acted as effective horizontal drains, significantly accelerating consolidation.

4.3 Long-term creep settlement

Using C_α/C_c = 0.03, the secondary settlement over 50 years after hydro-test was estimated at 30-50 mm in lower-bound and upper-bound conditions. This is well within the 250 *mm* tolerance of the flexible hoses. Figure 19 shows the predicted average creep settlement versus time. The secondary settlement follows a logarithmic time function.

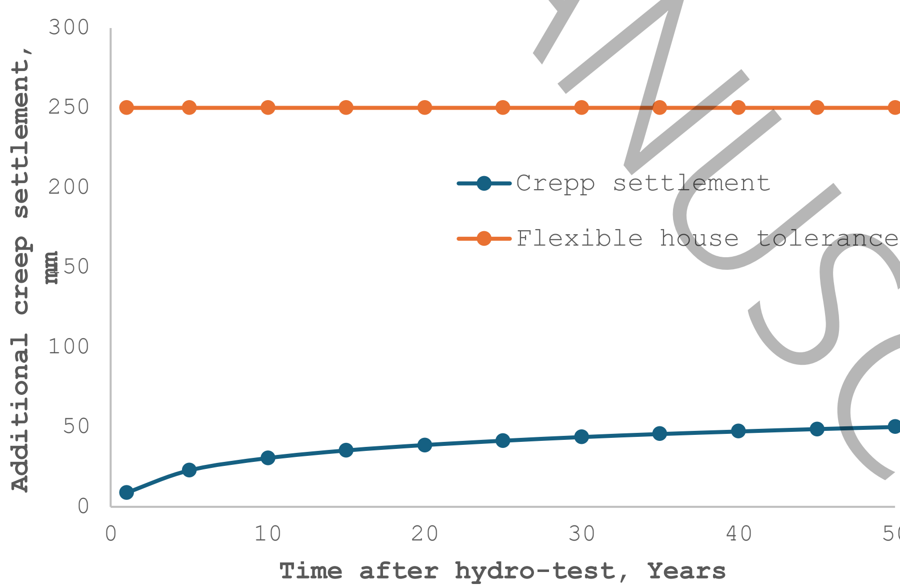

Fig. 19. Creep settlement curve over 50 years

4.4 Deficiencies and practical lessons

Access ladder connections: the ladders between adjacent tanks were rigidly welded. Because of differential settlement, the upper parts of the tanks moved closer together than the lower parts, causing out-of-plane buckling. In future projects, sliding restraints should be used for ladder connections. Figure 20 illustrates the upper ladder and flexible hose.

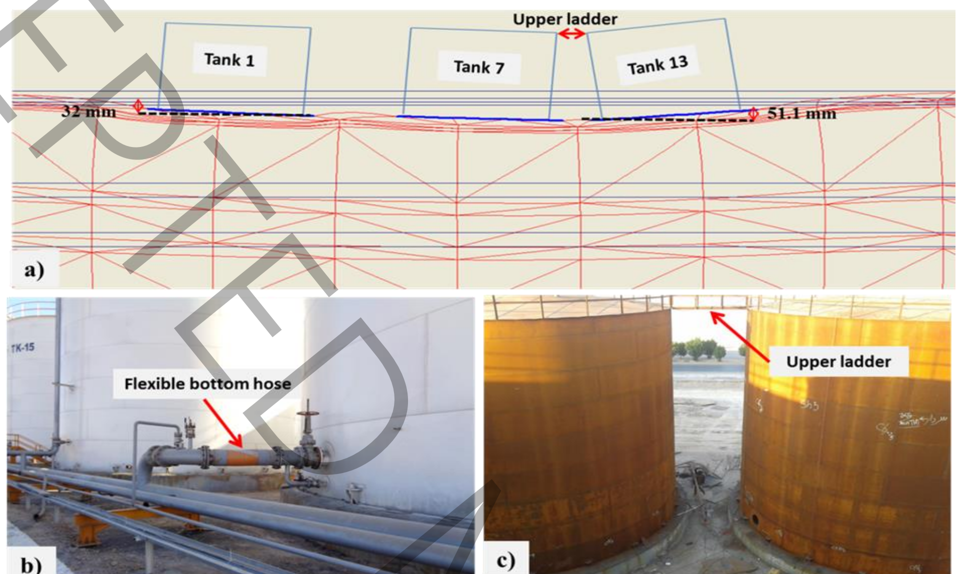

Fig. 20. Vertical settlement of tanks; a) differential settlement in North-South direction, b) using a flexible hose in the bottom of tanks to tolerate differential settlement, c) upper ladder for accessing the roof of tanks

5. Conclusions

This case study investigates constructing 18 steel tanks with 2000 m^3 capacity in Bandar Imam Port, southwest of Iran. Most soils beneath the steel tanks were loose clay soil with high consolidation settlement. Constructing a deep foundation or other ground improvement methods imposed high costs and construction time for this case study. Therefore, this case study was designed with an observational method to omit deep foundations and other ground improvement methods. For this purpose, shallow soil replacement was conducted to prevent general shear failure of the infrastructure, and with some effective techniques, the settlement of the tanks was tolerated. Conclusions of this study include the following.

- The formal observational method (with predefined trigger levels and contingency plans) successfully avoided deep foundations on a site where the imposed stress (164 *kPa*) was 4.5 times the settlement-controlled allowable pressure (36 *kPa*). No general shear failure occurred.

▪ A combination of 2 m engineered soil replacement (sand, GP, GM) and a 4-month-controlled hydro-test reduced total settlement from an estimated 380 *mm* (without preloading) to an average final settlement of 234 *mm*. The FEM prediction of 209 *mm* was within 12% of the field average.

▪ Horizontal silty interlayers (ML) at depths of 1.5–3 *m*, 13–16 *m*, and 30–34 *m* accelerated primary consolidation, reducing the required preloading time by approximately 30% compared to homogeneous clay.

▪ Long-term average creep after hydro-test was 30–50 *mm* over 50 years, which is well within the tolerance of flexible polyethylene hoses (250 *mm*).

▪ Practical recommendations for similar projects:

- Use flexible hoses for all pipe connections between tanks.
- Install sliding restraints for access ladders to accommodate differential settlement.
- Respect the full hydro-test schedule; do not accelerate filling despite client pressure.

Notation

The following symbols are used in the paper:

γ_d: dry unit weight

γ_w: wet unit weight

CL: Clay with low plasticity

C.B.R.: California Bearing Ratio test

ML: Silt with low plasticity

GM: Gravel materials

LL: Liquid Limit

PI: Plastic Index

c`: Drained cohesion

φ`: Drained internal friction angle

C_{uu}: Unconsolidated undrained

φ_{uu}: Unconsolidated undrained internal friction angle

W_n: Natural water content

e_0: Initial void ratio

Cc: Compression coefficient

Cr: Recompression coefficient

SPT: Standard Penetration Test

σ: Stress at the bottom of the foundation

D_f: Depth of foundation

Acknowledgments

The authors thank the geotechnical and construction teams at the Imam Khomeini port site for their diligent monitoring work, and the private operating company for financial support.

References

[1] API-650, American Petroleum Institute (API) Standard 650: "Welded steel tanks for oil storage", in, (2020).
[2] O.O. Agboola, B.O. Akinnuli, B. Kareem, M.A. Akintunde, Optimum detailed design of 13,000 m3 oil storage tanks using 0.8 height-diameter ratio, Materials Today: Proceedings, 44 (2021) 2837-2842.
[3] M. Hassanzadeh, K. Rahmani, Hydrostatic test of storage tanks using seawater and corrosion considerations, Engineering Failure Analysis, 122 (2021) 105267.
[4] R. Alipour, J. Khazaei, M.S. Pakbaz, A. Ghalandarzadeh, Settlement control by deep and mass soil mixing in clayey soil, Proceedings of the Institution of Civil Engineers - Geotechnical Engineering, 170(1) (2016) 27-37.
[5] R.B. Peck, Advantages and limitations of the observational method in applied soil mechanics, Géotechnique, 19(2) (1969) 171-187.
[6] Q. Li, Y. Li, S. Dong, Y. Mizukami, J. Han, T. Yoshida, D. Kitazawa, Performance and feasibility study of a novel automated catch-hauling device using a flexible hose net structure in set-net, Journal of Marine Science and Engineering, 9(9) (2021) 1015.
[7] M.S. Pakbaz, R. Alipour, Influence of cement addition on the geotechnical properties of an Iranian clay, Applied Clay Science, 67-68 (2012) 1-4.

[8] S.G. Chung, H.J. Kweon, Prediction of radial consolidation settlement with consideration of sampling range effect: updated observational methods, Journal of Geotechnical and Geoenvironmental Engineering, 147(12) (2021) 04021151.
[9] Eurocode7, geotechnical design–Part 1: general rules, British Standards: London, UK, (2004).
[10] W. Bjureland, J. Spross, F. Johansson, A. Prästings, S. Larsson, Reliability aspects of rock tunnel design with the observational method, International Journal of Rock Mechanics and Mining Sciences, 98 (2017) 102-110.
[11] J. Spross, F. Johansson, When is the observational method in geotechnical engineering favourable, Structural Safety, 66 (2017) 17-26.
[12] J.B. Serra, L. Miranda, Ground uncertainty implications in the application of the observational method to underground works: comparitive examples, in: Foundation Engineering in the Face of Uncertainty: Honoring Fred H. Kulhawy, (2013), pp. 254-270.
[13] K. Jones, M. Sun, C. Lin, Integrated analysis of LNG tank superstructure and foundation under lateral loading, Engineering Structures, 253 (2022) 113795.
[14] V. Balakumar, M.J. Huang, E. Oh, R. Hwang, A.S. Balasubramaniam, Piled raft on sandy soil- an extensive study, Geotechnical Engineering, 50(3) (2019) 136.
[15] R. Berardi, R. Lancellotta, Yielding from field behavior and its influence on oil tank settlements, Journal of Geotechnical and Geoenvironmental Engineering, 128(5) (2002) 404-415.
[16] D.T. Bergado, P. Jamsawang, P. Jongpradist, S. Likitlersuang, C. Pantaeng, N. Kovittayanun, F. Baez, Case study and numerical simulation of PVD improved soft Bangkok clay with surcharge and vacuum preloading using a modified air-water separation system, Geotextiles and Geomembranes, 50(1) (2022) 137-153.
[17] A.V. Govindasamy, J.-L. Briaud, D. Kim, F. Olivera, P. Gardoni, J. Delphia, Observation method for estimating future scour depth at existing bridges, Journal of Geotechnical and Geoenvironmental Engineering, 139(7) (2013) 1165-1175.
[18] L. Matešić, I. Mihaljević, G. Grget, P. Kvasnička, The use of hydro test results for design of steel tanks on stone column improved ground-a case history, in: Proceedings of the 18 th International Conference on Soil Mechanics and Geotechnical Engineering, Paris, (2013), pp. 579-582.
[19] T. Miranda, D. Dias, M. Pinheiro, S. Eclaircy-Caudron, Methodology for real-time adaptation of tunnels support using the observational method, Geomechanics and Engineering, 8(2) (2015) 153-171.
[20] A. Prästings, R. Müller, S. Larsson, The observational method applied to a high embankment founded on sulphide clay, Engineering Geology, 181 (2014) 112-123.
[21] J. Spross, F. Johansson, L.K.T. Uotinen, J.Y. Rafi, Using observational method to manage safety aspects of remedial grouting of concrete dam foundations, Geotechnical and Geological Engineering, 34(5) (2016) 1613-1630.
[22] H. Alielahi, M. Maleki, K. Mehrshahi, Performance evaluation of a surcharge preloading project based on back-analysis of field monitoring and numerical assessment, Arabian Journal of Geosciences, 14(21) (2021) 2162.
[23] A. 1994, Test method for bearing capacity of soil for static load on spread footings, D 1194-94, Annual Book of ASTM Standards, 4.08, in, American Society for Testing and Materials, West Conshocken, PA, USA, (1994).

[24] H.S. Al-Jubair, S.A. Abbas, A.A. Al-Mutar, Finite element analysis of a soft cohesive soil improved by column-like elements, International Journal of Geotechnical Engineering, 15(4) (2021) 418-432.